Lawrence Berkeley National Laboratory
Lawrence Berkeley National Laboratory

Title

Plasma wakefields driven by an incoherent combination of laser pulses: a path towards high-average power laser-plasma accelerators

Permalink

Author

Benedetti, C

Publication Date

2014-05-30

DOI

Plasma wakefields driven by an incoherent combination of laser pulses: a path towards high-average power laser-plasma accelerators

C. Benedetti,[1] C. B. Schroeder,[1] E. Esarey,[1] and W. P. Leemans[1]

Lawrence Berkeley National Laboratory, Berkeley, California 94720, USA

The wakefield generated in a plasma by incoherently combining a large number of low energy laser pulses (i.e., without constraining the pulse phases) is studied analytically and by means of fully-self-consistent particle-in-cell simulations. The structure of the wakefield has been characterized and its amplitude compared with the amplitude of the wake generated by a single (coherent) laser pulse. We show that, in spite of the incoherent nature of the wakefield within the volume occupied by the laser pulses, behind this region the structure of the wakefield can be regular with an amplitude comparable or equal to that obtained from a single pulse with the same energy. Wake generation requires that the incoherent structure in the laser energy density produced by the combined pulses exists on a time scale short compared to the plasma period. Incoherent combination of multiple laser pulses may enable a technologically simpler path to high-repetition rate, high-average power laser-plasma accelerators and associated applications.

I. INTRODUCTION

Plasma-based accelerators have received significant theoretical and experimental interest in the last years because of their ability to sustain extremely large acceleration gradients, enabling compact accelerating structures[1,2]. In a laser plasma accelerator (LPA), a short and intense laser pulse propagating in an underdense plasma, ponderomotively drives an electron plasma wave (or wakefield). The plasma wave has a relativistic phase velocity (of the order of the group velocity of the laser driver) and can support large accelerating and focusing fields. The relativistic plasma wave is the result of the gradient in laser field energy density providing a force (i.e., the ponderomotive force) that creates a space charge separation between the plasma electrons and the neutralizing ions. For a resonant laser pulse driver, i.e. with a length $L_0 \sim k_p^{-1}$, where $k_p = \omega_p/c$, c being the speed of light in vacuum and $\omega_p = (4\pi n_0 e^2/m)^{1/2}$ the electron plasma frequency for a plasma with density n_0 (m and e are, respectively, the electron mass and charge), with a relativistic intensity, i.e. with a normalized vector potential $a_0 = eA_0/mc^2 \sim 1$ (A_0 is the peak amplitude of the laser vector potential), the amplitude of the accelerating field is of order $E_0 = mc\omega_p/e$, or $E_0[\text{V/m}] \simeq 96\sqrt{n_0[\text{cm}^{-3}]}$. For instance, in a plasma with $n_0 \sim 10^{17}$ e/cm³, accelerating gradients on the order of ~ 30 GV/m can be obtained. This value is several orders of magnitude higher than in conventional accelerators, presently limited to gradients on the order of ~ 100 MV/m. LPAs have produced $\gtrsim 1$ GeV electron beams over a few centimeters plasmas with per-cent-level energy spread[3,4], and significant effort has been put to increase their reliability and tunability[5–9], and to fully characterize the properties of the laser-plasma accelerated beams[10–13].

The rapid development and properties of LPAs makes them interesting candidates for applications to future compact radiation sources[14–18] and high energy linear colliders[19–21]. However, significant laser technology advances are required to realize, for instance, a linear collider based on LPA techniques. A concept for a 1 TeV center-of-mass electron-positron LPA-based linear collider is presented in Ref. 20. A possible scenario foresees, for both the electron and positron arms, multiple LPA stages with a length of $L_{stage} \sim 1$ m, operating at a density of the order $n_0 \sim 10^{17}$ e/cm³. Each LPA stage is powered by a resonant laser pulse with duration $T_0 \sim L_0/c \lesssim 100$ fs, wavelength $\lambda_0 \sim 1$ μm, containing tens of Joules of laser energy (with a peak power of $\lesssim 1$ PW), and with a laser spot size $w_0 \sim \lambda_p = 2\pi/k_p$, yielding an intensity such that $a_0 \sim 1$, and creating a quasi-linear wake in the plasma with accelerating gradient $\sim E_0$. After propagating in a plasma stage the laser pulse driver is depleted. The accelerated particle bunches are then extracted form the plasma stage and re-injected in a subsequent LPA stage, powered by a new laser pulse, for further acceleration. The required laser intensities and energies are achievable with present laser technology. However, luminosity requirements dictate that the laser repetition rate is $f_{rep} \sim 10$ kHz (average laser power of hundreds of kW), which is orders of magnitude beyond present technology. The required repetition rate depends on the plasma density choice and scales as $f_{rep} \propto n_0$.[20] However, operating at a lower plasma density[21] reduces the accelerating gradient and increases beamstrahlung effects[22].

To date, LPAs are typically driven by solid-state (e.g., Ti:sapphire) lasers that are limited to an average power ~ 100 W. For example, the Berkeley Lab Laser Accelerator (BELLA) laser delivers 40 J pulses on target at 1 Hz[23]. Since virtually all applications of LPAs will benefit greatly from higher repetition rates, it is essential that high average power laser technology continues to be developed. Together with the increase in average laser power, the laser wall-plug efficiency will need to increase. Increasing the laser average power and efficiency would also benefit several future accelerator applications beyond LPAs, owing to the broad use of laser technology in

modern high performance accelerator facilities (e.g., driving electron/ion sources, pump and probe beams, seeding x-ray lasers, exciting matter into exotic non-equilibrium states, dielectric laser accelerators, lasers for Compton scattering sources, *etc.*)[24,25].

Several laser technologies are being studied and considered as potential candidates to provide systems with high average power and high wall-plug efficiency, namely, fiber lasers, diode-pumped solid-state lasers, and optical parametric chirped pulse amplification (OPCPA) based lasers[2,24–26]. For example, in Refs. 26 and 27, a scheme is presented were a large number of diode-pumped fiber systems, delivering pulses with $\sim$ mJ energy at kHz repetition rate, are combined in such a way that the relative phases of the output beams are controlled so they constructively interfere (coherent combination) and produce a single, high power output beam with high efficiency. The challenges in controlling individual phases are related not only to the large number of fibers to combine in order to achieve high peak power (e.g., $\sim 10^4$ fibers for a ~ 30 J energy pulse), but also to the fact that coherent combination of pulsed beams with a duration of a few tens or hundreds of femtoseconds requires matching of both phase and group delays using phase modulators and delay lines. So far, the coherent combination of an array of 64 (continuous wave) beams from fiber amplifiers with $\lambda_0/60$ precision has been demonstrated[28]. The coherent combination of a small number of femtoseconds lasers has also been achieved[29,30].

In this paper we show that an LPA does not require a fully coherent driver laser pulse. This is true because the LPA wakefield is excited by the ponderomotive force (i.e., the gradient in the electromagnetic energy density), along with the fact that the plasma responds on the time scale λ_p/c. Large amplitude wakefield excitation requires sufficient electromagnetic energy within a given volume, typically of the order of $\sim \lambda_p^3$. Since the wakefield response behind the driver depends on the time-integrated behavior of the electromagnetic energy density of the driver over λ_p/c, it is insensitive to time structure in the driver on time scales $\ll \lambda_p/c$, which allows for the use of incoherently combined laser pulses as the driver. Theoretically, this can be easily demonstrated in the linear ($a^2 < 1$) wakefield regime in which the amplitude of the electric field of the wake is small ($|\mathbf{E}|/E_0 < 1$). In the linear regime, the wake electric field $\mathbf{E}$ is given by[1]

$$\left(\partial^2/\partial t^2 + \omega_p^2\right) \mathbf{E}/E_0 = -(c\omega_p/2)\nabla a^2, \qquad (1)$$

with the solution

$$\mathbf{E}/E_0 = -(c/2) \int_0^t dt' \sin[\omega_p(t - t')]\nabla a^2(t'). \qquad (2)$$

This Green function solution averages out the small scale time structure in the ponderomotive force. Hence, in effect, the wakefield is given by

$$\left(\partial^2/\partial t^2 + \omega_p^2\right) \mathbf{E}/E_0 \simeq -(c\omega_p/2)\nabla \langle a^2 \rangle, \qquad (3)$$

where the angular brackets represent a time average over scales small compared to λ_p/c.

Owing to the time average process characterizing the wake excitation, we show that multiple, low-energy, incoherently combined laser pulses can deposit sufficient field energy in the plasma to ponderomotively drive a large wakefield. We show that no phase control in the combination of multiple laser pulses is required for LPAs. We find that, under certain conditions, the wake generated by an incoherent combination of pulses is regular behind the driver and its amplitude is comparable, or equal, to the one obtained by using a single coherent pulse with the same energy. We expect that the fundamental requirements to achieve incoherent combination are more relaxed compared to coherent combination. Hence, incoherent combination may provide an alternative and technically simpler path to the realization of high repetition rate and high average power LPAs.

In this paper we analyze, analytically and numerically by means of fully-self-consistent particle-in-cell (PIC) simulations, the wakefield generated in a plasma by combining a large number of low energy laser pulses without constraining the phases of the different laser pulses (incoherent combining). To illustrate the physics of wake generation using multiple, incoherent pulses, we consider, as examples, three different incoherent combination schemes: (1) spectral combining (where different laser pulses, spectrally separated, are spatially overlapped by using a dispersive optical system), (2) short pulse stacking (where short pulses with a moderately low energy but high intensity are stacked longitudinally), and (3) a mosaic of beamlets (where short and narrow laser pulses are placed side-by-side tiling a prescribed volume). We show that, in spite of the (in general) incoherent nature of the wakefield within the volume occupied by the laser pulses, behind this region the structure of the wakefield is, in some cases, completely regular, and its amplitude is comparable or equal to the one obtained by using a single (coherent) pulse with same energy. We also characterize the evolution of the wakefield as the incoherent combination of pulses propagates in the plasma. The results are of interest for high-repetition rate LPA applications, such as an LPA-based collider.

The paper is organized as follows. Wakefield excitation using the spectral combining scheme is presented in Sec. II, the pulse stacking method in Sec. III, and the mosaic of beamlets in Sec. IV. Conclusions are presented in Sec. V.

II. SPECTRAL COMBINATION OF INCOHERENT PULSES

Although technically difficult to realize, we consider the idealized case of spectrally combining a large number of incoherent pulses to demonstrate the principal that wakefield excitation does not require the energy density of the driver to be in a single coherent pulse. We con-

sider a collection of N laser pulses propagating along the longitudinal direction, z, in a parabolic plasma channel. The plasma density profile is given by

$$n(r) = n_0 + \frac{1}{\pi r_e r_0^2} \left(\frac{r}{r_0}\right)^2, \qquad (4)$$

where n_0 is the on-axis ($r = \sqrt{x^2 + y^2} = 0$) plasma density, r_0 determines the channel depth, and $r_e = e^2/mc^2 \simeq 2.82 \times 10^{-13}$ cm is the classical electron radius. For convenience throughout the paper we will use comoving coordinates, namely $\zeta = z - ct$, $s = ct$. Each (linearly polarized) laser pulse is described initially ($s = 0$) by a transverse normalized laser vector potential of the form

$$a_{\perp,j}(\boldsymbol{r}, \zeta) = a_{0,j} \exp\left(-\frac{\boldsymbol{r}^2}{w_0^2}\right) \exp\left(-\frac{\zeta^2}{L_0^2}\right) \cos(k_{0,j}\zeta + \varphi_j), \qquad (5)$$

for $j = 1, \cdots, N$, where $a_{0,j}$ is the amplitude of the laser vector potential for the j−th laser pulse, $k_{0,j} = 2\pi/\lambda_{0,j}$ is the wavenumber associated with the laser wavelength $\lambda_{0,j}$, φ_j is an arbitrary (random) phase, w_0 and L_0 are, respectively, the laser spot size and pulse length (for simplicity we assume all the lasers have the same spot size and pulse length, we also assume that $k_{0,j}w_0 \gg 1$ and $k_{0,j}L_0 \gg 1$, for $j = 1, \cdots, N$). Denoting by $I_{0,j}$ the laser peak intensity, then $a_{0,j} \simeq 8.5 \cdot 10^{-10}(I_{0,j}[\text{W/cm}^2])^{1/2}\lambda_{0,j}[\mu m]$. We consider pulse lengths such that $L_0 \sim k_p^{-1}$ (resonant laser pulses), where k_p is the plasma wave number corresponding to the on-axis density n_0. If we take $w_0 = r_0$, every laser pulse is (linearly) matched in the channel and so, in the limit of low-power and low-intensity, its spot size does not evolve during propagation. Under these conditions we expect each pulse to propagate in the channel with a constant group velocity $v_{g,j}$ (neglecting nonlinear effects such as self-steepening and depletion[32]) given by[33]

$$\beta_{g,j} = \frac{v_{g,j}}{c} \simeq 1 - \frac{k_p^2}{2k_{0,j}^2} - \frac{2}{k_{0,j}^2 r_0^2}. \qquad (6)$$

To leading order, the transverse laser field, which is the dominant component for a broad pulse, is $E_{\perp,j} \simeq (mc^2/e)\partial_\zeta a_{\perp,j}$. We define the (denormalized)

laser pulse energy as $U_j = \int d\zeta \int 2\pi r dr\, (\partial_\zeta a_{\perp,j})^2 \simeq (\pi/2)^{3/2}a_{0,j}^2 k_{0,j}^2 w_0^2 L_0/2$. We also assume that the N laser pulses are spectrally separated, namely, the power spectra of the pulses do not overlap with each other (wavelength combining). The spectral bandwidth of each pulse (Gaussian longitudinal profile) can be estimated as $\Delta k \sim 1/L_0$, so the condition of spectral separation can be expressed as

$$|k_{0,j} - k_{0,l}| \gg \Delta k \sim 1/L_0, \qquad (7)$$

for $j \neq l$, and the following condition also holds,

$$\int_{-\infty}^{+\infty} d\zeta\, F(\zeta)\, a_{\perp,j}(\boldsymbol{r}, \zeta) a_{\perp,l}(\boldsymbol{r}, \zeta) = 0, \qquad (8)$$

for $j \neq l$, where $F(\zeta)$ is any slowly varying function, namely $|\partial_\zeta F| \lesssim |F|/L_0$. The total energy of the combination is then simply

$$U_{tot} = \sum_{j=1}^{N} U_j = \frac{1}{2}\left(\frac{\pi}{2}\right)^{3/2} w_0^2 L_0 \sum_{j=1}^{N} a_{0,j}^2 k_{0,j}^2. \qquad (9)$$

From an experimental point of view, the condition of spectral separation allows the overlap of N different beams by using a dispersive optical system like a sequence of dichroic mirrors, a grating, or a prism[31]. To compute the wakefield generated by the combination of laser pulses requires solving Maxwell's equations coupled with the cold plasma fluid equations. Assuming that individual plasma particles are passed over by the laser pulses and the associated wake in a short time compared with the time over which the shape of the laser pulses or the wake evolve, we can make the quasi-static approximation, i.e. $\partial_s \simeq 0$ in all the wake quantities. Denoting by ϕ_{tot} the wake potential (normalized to mc^2/e), we have[1]

$$\frac{1}{k_p^2}\frac{\partial^2 \phi_{tot}}{\partial \zeta^2} = -\phi_{tot} + \frac{a_{tot}^2}{2}, \qquad (10)$$

where $a_{tot} = \sum_j a_{\perp,j}$. Eq. (10) is valid in the limit of a broad plasma channel, $k_p^2 r_0^2 \gg 1$, and low intensity, $a_{tot} \lesssim 1$ (linear wakefield). The longitudinal accelerating field is then $E_z/E_0 = -\partial\phi_{tot}/\partial(k_p\zeta)$. The Green function solution to Eq. (10) is

$$\phi_{tot}(\boldsymbol{r}, \zeta) = -\sin(k_p\zeta)\int_\zeta^\infty d(k_p\zeta')\cos(k_p\zeta')\frac{a_{tot}^2(\boldsymbol{r}, \zeta')}{2} + \cos(k_p\zeta)\int_\zeta^\infty d(k_p\zeta')\sin(k_p\zeta')\frac{a_{tot}^2(\boldsymbol{r}, \zeta')}{2}, \qquad (11)$$

where

$$a_{tot}^2 = \sum_{j=1}^{N} a_{\perp,j}^2 + \sum_{j=1}^{N}\sum_{l=1,l\neq j}^{N} a_{\perp,j}a_{\perp,l}. \qquad (12)$$

The solution for wake phases ζ in the domain following

the pulses where all the laser fields vanish is obtained by taking the limit $\zeta \to -\infty$ in the integrals of Eq. (11). By inserting Eq. (12) in Eq. (11) and using the spectral separation condition Eq. (8) (in our case $k_pL_0 \sim 1$, then the functions $\cos(k_p\zeta')$ and $\sin(k_p\zeta')$ within the integrals are slowly varying functions) we find that the contribu-

tions to the integrals coming from the double summation (i.e., the terms with $j \neq l$) are vanishing. The wakefield potential behind the laser pulses then reads

$$\phi_{tot} \simeq -\frac{1}{4}\sqrt{\frac{\pi}{2}}(k_p L_0)e^{-(k_p L_0)^2/8}e^{-2r^2/w_0^2}\sin k_p\zeta \sum_{j=1}^{N} a_{0,j}^2,$$ (13)

where we used the assumption $k_{0,j}L_0 \gg 1$ to perform an average over the fast laser oscillations on each of the terms $a_{\perp,j}^2$ originating from the first sum in Eq. (12). The average removes the dependence of ϕ_{tot} on the laser phases φ_j. We notice that for wake phases within the volume occupied by the lasers, where we cannot take the limit $\zeta \to -\infty$ in the integrals of Eq. (11), the contribution to the wakefield originating from the interference between the lasers [double summation term in Eq. (12)] does not vanish, yielding an "incoherent" behavior for ϕ_{tot} characterized by the non-smoothness of the wakefield due to the presence of spatial structures at several different spatial scales and by the fact that these structures depend on the particular values of the relative laser phases $\varphi_j - \varphi_l$.

We consider now the wakefield generated by a single ("coherent") bi-Gaussian, linearly polarized laser pulse [same form for the vector potential as in Eq. (5)] and with the same pulse length, L_0, and spot size, w_0, as before. We denote by A_0 the amplitude of the normalized vector potential, and by $\lambda_0 = 2\pi/K_0$ the laser wavelength. Also in this case we assume $K_0 L_0 \gg 1$ and $K_0 w_0 \gg 1$. The (denormalized) pulse energy is $U_c = (\pi/2)^{3/2}A_0^2 K_0^2 w_0^2 L_0/2$ and the expression of the wake potential in the region behind the laser driver is

$$\phi_c \simeq -\frac{A_0^2}{4}\sqrt{\frac{\pi}{2}}(k_p L_0)e^{-(k_p L_0)^2/8}e^{-2r^2/w_0^2}\sin k_p\zeta. \quad (14)$$

Equating the laser energy and the wakefield amplitude for the single pulse to the corresponding quantities in the case of N pulses incoherently combined, namely Eq. (9) and Eq. (13), we obtain the following consistency conditions

$$\begin{cases} \sum_{j=1}^{N} a_{0,j}^2 k_{0,j}^2 = A_0^2 K_0^2, & \text{(equal energy)} \\ \sum_{j=1}^{N} a_{0,j}^2 = A_0^2, & \text{(equal wakefield)}. \end{cases} \quad (15)$$

Therefore, given a set of spectrally separated, low power laser pulses with identical pulse lengths and spot sizes, and with wavenumbers and amplitudes of the normalized vector potential satisfying Eq. (15), the wakefield generated in a plasma channel by their (incoherent) combination equals, in the region behind the pulses, the one generated by a single laser pulse with the same total energy, pulse length and spot size.

We notice, however, that this equivalence applies only in the early stages of the laser plasma interaction. In fact, during propagation, owing to the fact that lasers with different frequencies are characterized by different group velocities as expressed in Eq. (6), the combination

of pulses disperses and, consequently, the amplitude of the excited wake drops. We can estimate the lengthening of the laser driver due to dispersion as follows. We denote by $k_{min}, \overline{k}$, and k_{max}, respectively, the minimum, central, and maximum laser wavenumbers in the combination, we also define $\delta k = k_{max} - k_{min}$, then, using Eq. (6), the rate at which the lasers disperse is

$$\delta L \sim [\beta_g(k_{max}) - \beta_g(k_{min})]s \sim \left[\left(\frac{k_p}{\overline{k}}\right)^2 + \frac{4}{(\overline{k}r_0)^2}\right]\frac{\delta k}{\overline{k}}s. \quad (16)$$

The driver loses resonance with the plasma when $(k_p\delta L)^2 \gg 1$, causing a reduction of the wakefield amplitude. For the case where the driver loses resonance and the laser pulses are not fully depleted, some (or all) of their remaining energy may be recovered when the lasers exit the plasma channel.

The consistency conditions Eq. (15) can be fulfilled in several ways. In the following we present two examples. In the first one we consider a set of laser pulses with the same normalized laser vector potential and different energies. In the second one we consider a set of pulses with the same energy and different values for the normalized vector potential. In both cases, we assume that the laser wavenumbers are given by

$$k_{0,j}/K_0 = \alpha + \beta j, \quad (17)$$

for $j = 1, \cdots, N$, where β, which sets the spectral separation between lasers pulses, is fixed in such a way the condition expressed in Eq. (7) is satisfied, namely $|k_{0,j+1}-k_{0,j}| = K_0\beta \gg 1/L_0 \sim k_p$, implying $\beta \gg k_p/K_0$, and α depends on the number of laser pulses and on the particular laser combination scheme as explained below.

For the case of pulses with the same normalized laser vector potential we have $a_{0,j} = A_0/\sqrt{N}$, and the second condition in Eq. (15) is automatically satisfied, while the first one, together with Eq. (17), gives

$$\alpha^2 + \alpha\beta(N+1) + \frac{\beta^2}{6}(2N^2 + 3N + 1) - 1 = 0. \quad (18)$$

Solving for α in Eq. (18) we finally determine the values of $k_{0,j}$ to be used in the laser combination. We notice, however, that a solution does not exist for an arbitrarily large number of lasers. For this particular scheme we have $N \lesssim (\sqrt{1 + 48/\beta^2} - 3)/4$ (with $\beta < \sqrt{6}$), or, in the limit $\beta \ll 1$, $N \lesssim \sqrt{3}/\beta$. For instance, in a 10 GeV LPA stage powered by a BELLA-type laser ($U_c \sim 30$ J, $\lambda_0 \sim 1$ μm, $A_0 \sim 1$), we have $k_p/K_0 \sim 0.01$. Choosing $\beta \sim 0.08$, we obtain that the maximum number of lasers that can be accommodated with this scheme is $N \sim 20$, and so $a_0 \sim 0.22$. The minimum and maximum laser wavelengths are, respectively, 0.6 μm and 8.9 μm, and the corresponding laser energies are 4 J, and 20 mJ. This scheme is characterized by a strong imbalance among the energies of the different beams.

As a second example, we consider pulses of equal energy. We have $a_{0,j}k_{0,j} = A_0 K_0/\sqrt{N}$, and, in this case,

the first condition in Eq. (15) is automatically satisfied. We also have $a_{0,j} = (A_0/\sqrt{N})K_0/k_{0,j} = (A_0/\sqrt{N})(\alpha + \beta j)^{-1}$, and using the second condition in Eq. (15) we obtain the equation for α for this configuration of lasers, namely

$$\sum_{j=1}^{N} \frac{1}{(\alpha + \beta j)^2} = N. \tag{19}$$

The maximum number of lasers that can be accommodated in this case is, in the limit $\beta \ll 1$, $N \lesssim 1.6/\beta^2$, so this configuration shows a more favorable scaling with β compared to the equal amplitude combination scheme. In fact, if we take, as before, $k_p/K_0 \sim 0.01$ (e.g., 10 GeV LPA stage) and $\beta \sim 0.08$, we obtain that the maximum number of lasers is $N \sim 250$. The energy of each pulse is then ~ 120 mJ, the minimum and maximum laser wavelengths to be used in the combination are, respectively, 12 μm (with $a_0 = 0.78$) and 0.05 μm (with $a_0 = 0.0031$). We recall that, however, the larger is the number of beams, and so the larger is the range of laser wavelengths employed, the fastest the pulse combination will disperse. More specifically, according to Eq. (16), since $\delta k = k_{max} - k_{min} \propto N$, we have that the propagation length over which the combination disperses is $\propto 1/N$. Finally, we note that, in both examples, we can accommodate twice the number of laser pulses (and so decrease the laser energy of each pulse) without increasing the range of laser wavelengths, by considering polarization multiplexing.

A numerical example of wakefield generated by a spectral combination of incoherent pulses is presented in Fig. (1). In Fig. (1) (a) we show (red line) the normalized laser field, $a(\zeta)$, generated by incoherently combining 50 spectrally separated laser pulses with equal energies. The black dashed line is the laser envelope for a single (coherent) laser pulse with $A_0 = 1.5$, $K_0/k_p = 150$, and $k_p L_0 = 2$. The incoherent laser parameters, namely $k_{0,j}, a_{0,j}$, are chosen such that the conditions expressed by Eq. (15) hold. The laser phases are random. In Fig. (1) (b) we show the lineout of the longitudinal accelerating field, $E_z(\zeta)/E_0$, generated by the coherent pulse (black line) and by the incoherent combination of laser pulses for two different set of values of the laser phases (red and blue dashed lines). We notice that the wakefield from incoherent combination is regular behind the driver region, namely $k_p \zeta \lesssim -4$, its amplitude equals the one from the single coherent pulse with the same energy, and no dependence on the laser phases is observed. This is in contrast to the region within the driver ($|k_p \zeta| \lesssim 4$), where the wakefield shows, as expected, an "incoherent" pattern with dependence on laser phases.

So far, we considered the centroids of the spectrally separated laser pulses to be completely overlapped. However, if this is not the case, both the structure (shape) and the amplitude of the wakefield are different compared to the case where the centroids are superimposed. Denoting by (x_0, y_0, z_0) the coordinates of the centroid for a
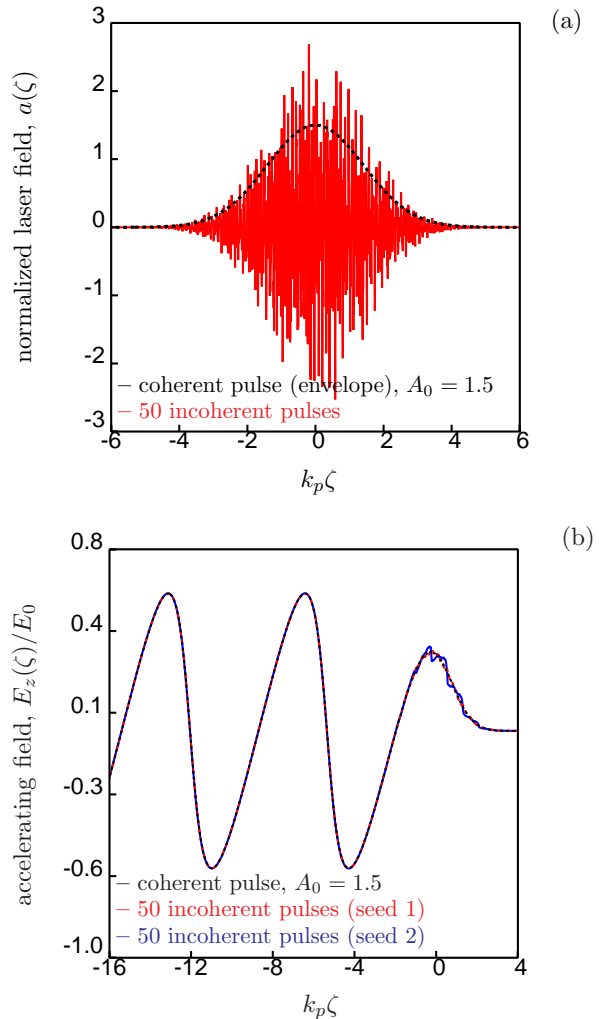

FIG. 1. (a) Normalized laser field generated by incoherently combining 50 spectrally separated laser pulses with equal energies (red line). The black dashed line is the laser envelope for a single (coherent) laser pulse with $A_0 = 1.5$, $K_0/k_p = 150$, and $k_p L_0 = 2$. The incoherent laser parameters, $k_{0,j}, a_{0,j}$, are chosen such that the conditions expressed by Eq. (15) hold. The laser phases are random. (b) Lineout of the longitudinal accelerating field generated by the coherent pulse (black line) and by the incoherent combination of laser pulses for two different set of values of the laser phases (red and blue dashed lines).

generic laser pulse, we assume that the centroids are randomly distributed with a Gaussian probability distribution function such that, initially, $\langle x_0 \rangle = \langle y_0 \rangle = \langle z_0 \rangle = 0$, $\langle x_0^2 \rangle = \langle y_0^2 \rangle = \sigma_\perp^2$, and $\langle z_0^2 \rangle = \sigma_z^2$. In general the centroid distribution will evolve during propagation, however, at least for short pulses in the low-power and low-intensity limit, it will maintain a Gaussian feature. This is due to the fact that the centroid of each laser which is, initially, off-axis or with a non-vanishing injection angle, performs harmonic oscillations about the channel axis
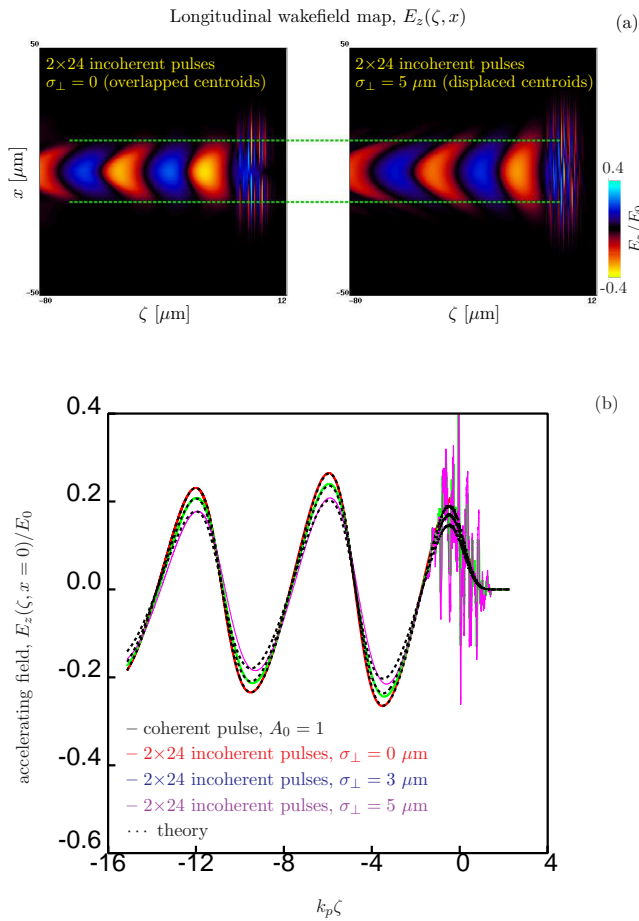
Longitudinal wakefield map, $E_z(\zeta, x)$ (a)

2×24 incoherent pulses
$\sigma_\perp = 0$ (overlapped centroids)

2×24 incoherent pulses
$\sigma_\perp = 5\ \mu m$ (displaced centroids)

(b)

- coherent pulse, $A_0 = 1$
- 2×24 incoherent pulses, $\sigma_\perp = 0\ \mu m$
- 2×24 incoherent pulses, $\sigma_\perp = 3\ \mu m$
- 2×24 incoherent pulses, $\sigma_\perp = 5\ \mu m$
- ⋯ theory

FIG. 2. (a) Snapshots of the longitudinal wakefield maps, $E_z(\zeta, x)$, generated by an incoherent combination of 48 spectrally separated pulses (including polarization multiplexing) with identical energies and with $\sigma_\perp = 0$ (overlapped centroids, left panel), and $\sigma_\perp = 5\ \mu m$ (displaced centroids, right panel). In both cases $\sigma_z = 0$ (no longitudinal centroids displacement). The laser and plasma parameters are $n_0 = 10^{18}$ cm^{-3}, $r_0 = w_0 = 12\ \mu m$, and $L_0 = 8\ \mu m$. The remaining incoherent laser parameters, namely $k_{0,j}, a_{0,j}$, are chosen such that the conditions expressed by Eq. (15) are satisfied with $A_0 = 1$ and $\lambda_0 = 0.8\ \mu m$. The green dashed lines delimit the transverse wakefield extent for the case with $\sigma_\perp = 0$. (b) On-axis lineout of the longitudinal accelerating field generated by a coherent pulse with $A_0 = 1$ (black solid line), and by the incoherent combination of 48 pulses with the same energy as the coherent pulse and centroid displacements such that $\sigma_\perp = 0$ (red), 3 μm (green), and 5 μm (purple). The black dotted lines correspond to the theoretical predictions for the on-axis lineout of the accelerating wakefield.

with a period $Z_{os} = 2\pi Z_m$, where $Z_m = k_0 r_0^2 / 2$. In particular, if the distribution of the injection angles (i.e., θ_x and θ_y) is chosen also to be Gaussian with, initially, $\langle \theta_x \rangle = \langle \theta_y \rangle = 0$, $\langle \theta_x^2 \rangle = \langle \theta_y^2 \rangle = \sigma_\perp^2 \langle Z_m^2 \rangle$, and all the other second order moments are vanishing, then the transverse centroid distribution is "matched" in the channel and all the second order moments of the distribution are con-

stant during propagation, for propagation lengths short compared to the characteristic dispersion length. Summing over the incoherent laser pulses distribution, the wakefield behind the pulses for non-overlapping laser centroids is

$$\phi_{tot} \simeq -\frac{A_0'^2}{4} \sqrt{\frac{\pi}{2}} (k_p L) e^{-(k_p L)^2/8} e^{-2r^2/w^2} \sin k_p \zeta, \quad (20)$$

where $L^2 = L_0^2 + 4\sigma_z^2$, $w^2 = w_0^2 + 4\sigma_\perp^2$, and

$$A_0'^2 = \frac{L_0}{L} \left(\frac{w_0}{w}\right)^2 \sum_{j=1}^N a_{0,j}^2 = \frac{L_0}{L} \left(\frac{w_0}{w}\right)^2 A_0^2. \quad (21)$$

We note that the wakefield structure is determined by the properties of the incoherent energy distribution. For instance, the transverse characteristic size of the wakefield increases from $\sim w_0$ to $\sim w$ in accordance with the increase in the transverse extent of the incoherent energy distribution due to transverse centroid displacement. Similarly, the effective driver length determining the wake excitation is the characteristic length of the incoherent energy distribution, L [i.e., wake excitation proportional to $(k_p L) e^{-(k_p L)^2/8}$]. Finally, we have that the effective driver field strength for wake excitation is reduced compared to the case where the centroids are overlapped, namely $A_0'^2/A_0^2 = (L_0/L)(w_0/w)^2 \leq 1$, and this is consistent with the fact that, by displacing the laser centroids, the total incoherent energy is distributed over a volume that is $(L/L_0)(w/w_0)^2$ times larger compared to the case where the centroids are overlapped.

In Fig. (2) (a) we show maps, obtained in 2D simulations with the PIC code ALaDyn[34,35], of the longitudinal wakefield, $E_z(\zeta, x)$, generated by an incoherent combination of 48 spectrally separated pulses (including polarization multiplexing) with identical energies and with $\sigma_\perp = 0$ (overlapped centroids, left panel), and $\sigma_\perp = 5\ \mu m$ (displaced centroids, right panel). In both cases $\sigma_z = 0$ (no longitudinal centroids displacement). The laser and plasma parameters are $n_0 = 10^{18}$ cm^{-3}, $r_0 = w_0 = 12$ μm, and $L_0 = 8\ \mu m$. The remaining incoherent laser parameters, namely $k_{0,j}, a_{0,j}$, are chosen such that the conditions expressed by Eq. (15) are satisfied with $A_0 = 1$ and $\lambda_0 = 0.8$ μm. The green dashed lines delimit the transverse wakefield extent for the case with $\sigma_\perp = 0$ (left panel). As anticipated, the characteristic transverse size of the wakefield is increased when the laser centroids are displaced.

In Fig. (2) (b) we show the on-axis lineout of the longitudinal accelerating field, $E_z(\zeta, x = 0)/E_0$, generated by a coherent pulse with $A_0 = 1$ (black solid line), and by the incoherent combination of 48 pulses with the same energy as the coherent pulse and centroid displacements such that $\sigma_\perp = 0$ (red), 3 μm (green) and 5 μm (purple). We note that the black (coherent pulse) and red (incoherent combination with $\sigma_\perp = 0$) solid curves are completely overlapped behind the driver region. The black dotted lines correspond to the theoretical predictions for the on-

axis lineout of the accelerating wakefield. More specifically, following Eq. (20) rewritten for the 2D Cartesian geometry, we have that the accelerating wakefield for the incoherent combination is expected to scale as

$$\frac{E_{z,\text{incoherent}}(\zeta, x=0)}{E_{z,\text{coherent}}(\zeta, x=0)} = \frac{w_0}{w} = \left(1 + \frac{4\sigma_\perp^2}{w_0^2}\right)^{-1/2}. \quad (22)$$

The theoretical prediction is in good agreement with the simulations.

III. INCOHERENT LASER PULSE STACKING

In this section, we consider N identical short laser pulses with high peak intensity and, owing to the short duration, moderately low energy, stacked longitudinally in a parabolic plasma channel as the one described by Eq. (4). All the linearly polarized laser pulses have the same amplitude of the normalized vector potential, a_0, wavelength, $\lambda_0 = 2\pi/k_0$, pulse length, ℓ_0, spot size, w_0, and independent (random) phases, φ_j. We assume $k_p\ell_0 \ll 1$ (short pulse compared to the plasma wavelength), $\ell_0 \gtrsim 2\lambda_0$, and $k_0 w_0 \gg 1$ (broad pulse). As before we take $w_0 = r_0$ so every laser is (linearly) matched in the channel during propagation. The form of the laser vector potential for the pulses at $s = 0$ is

$$a_{\perp,j}(\boldsymbol{r}, \zeta) = a_0 \exp\left(-\frac{\boldsymbol{r}^2}{w_0^2}\right) f\left(\frac{\zeta - \zeta_{0,j}}{\ell_0}\right)$$
$$\times \cos[k_0(\zeta - \zeta_{0,j}) + \varphi_j], \quad (23)$$

for $j = 1, \cdots, N$, where $z_{0,j}$ is the longitudinal coordinate of the centroid for the j-th laser, and $f(y)$ is a compact support function describing the longitudinal envelope. In the following we will assume

$$f(y) = \begin{cases} \cos^2(\pi y), & |y| \leq \frac{1}{2}, \\ 0, & |y| > \frac{1}{2}. \end{cases} \quad (24)$$

The energy of each pulse, keeping into account the contribution of the finite length envelope, is

$$U_j \simeq \frac{3}{32}\pi a_0^2 k_0^2 w_0^2 \ell_0 \left[1 + \frac{4\pi^2}{3}\frac{1}{(k_0\ell_0)^2}\right]. \quad (25)$$

The laser pulses are located, longitudinally, one after the other (longitudinal stack of pulses) such that the separation between two adjacent pulses is ℓ_0 (well separated lasers), namely $|\zeta_{0,j+1} - \zeta_{0,j}| = \Delta\zeta = \ell_0$, in this case the total energy of the pulses is simply

$$U_{tot} = \sum_{j=1}^{N} U_j \simeq \frac{3}{32}\pi N a_0^2 k_0^2 w_0^2 \ell_0 \left[1 + \frac{4\pi^2}{3}\frac{1}{(k_0\ell_0)^2}\right]. \quad (26)$$

The concept of driving the wakefield with a long train of short pulses spaced by the plasma period has been studied[1], and has been recently re-examined as a technique for driving plasma accelerators with efficient, low-energy, high-repetition lasers[2]. However, some concern may be raised about the possibility that the wake remains coherent after several hundreds (or thousand) of plasma periods. Furthermore, using pulse trains, the fluctuations in the background density need to be small in order to avoid changes in the phase velocity of the wake due to variations of the plasma wavelength, $\lambda_p = 2\pi/k_p \propto 1/\sqrt{n_0}$, that could potentially spoil the properties or limit the energy gain of the accelerated bunch located at some phase (accelerating and focusing) behind the last laser pulse. In our approach all the pulses are located within a plasma period and we use the combined envelope of the stack of short, sub-resonant pulses to synthesize the envelope of a single longer, resonant pulse.

The wakefield, ϕ_{tot}, generated behind the train of N pulses can be compute analytically in the limit $a_0 \lesssim 1$ using, as before, the quasi-static approximation. We will also make the assumption of broad plasma channel, $k_p^2 r_0^2 \gg 1$. Owing to linearity of the wakefields and to the fact that the different pulses are non-overlapping, we have $\phi_{tot} = \sum_{j=1}^{N} \phi_j$ and ϕ_j, and the single-pulse contribution to the wakefield, satisfies $k_p^{-2}(\partial^2\phi_j/\partial\zeta^2) = -\phi_j + a_{\perp,j}^2/2$. The Green function solution for ϕ_j in the region behind the laser pulse where the laser field vanishes, namely $\zeta < \zeta_{0,j} - \ell_0/2$, is

$$\phi_j = -\frac{3}{32}a_0^2(k_p\ell_0)e^{-2r^2/w_0^2}\left\{\sin\left[k_p(\zeta - \zeta_{0,j})\right] + G\left(\frac{k_0\ell_0}{\pi}\right)\cos(2\varphi_j)\sin\left[k_p(\zeta + \zeta_{0,j})\right]\right\}, \quad (27)$$

where $G(x) = (4/\pi)[\sin\pi x/(4x - 5x^3 + x^5)]$. We notice that ϕ_j depends on the laser phase φ_j, however the function $G(k_0\ell_0/\pi)$ goes to zero quickly as L_0 increases ($|G| \sim 1/(k_0\ell_0)^5$ for $k_0\ell_0$ large). For instance, already if we take $\ell_0 \gtrsim 2\lambda_0$, then $G \lesssim 10^{-3}$, and so the dependence of the wakefield amplitude on the laser

phase can be neglected. Assuming the N lasers are distributed in the interval $-L_0/2 \leq \zeta \leq L_0/2$, that is $\zeta_{0,j} = -L_0/2 + \ell_0(j-1)/(N-1)$, for $j = 1, \cdots, N$, then the total wakefield in the region $\zeta < -L_0/2 - \ell_0/2$

is

$$\phi_{tot} = -\frac{3}{32}a_0^2(k_p\ell_0)\left(\sum_{j=1}^{N}\cos k_p\zeta_{0,j}\right)e^{-2\boldsymbol{r}^2/w_0^2}\sin k_p\zeta$$

$$\simeq -\frac{3}{16}a_0^2\sin\left(\frac{k_pL_0}{2}\right)e^{-2\boldsymbol{r}^2/w_0^2}\sin k_p\zeta, \qquad (28)$$

where we assumed $N \gg 1$.

We compare the wakefield generated by the stack of pulses with the one generated by a single (coherent) laser pulse with amplitude A_0, wavenumber k_0, spot size $w_0 = r_0$, and a longitudinal flattop intensity profile of length L_0, namely $a_c(\zeta, \boldsymbol{r}) = A_0\exp(-\boldsymbol{r}^2/w_0^2)\cos(k_0\zeta)$ for $|\zeta| < L_0/2$, for $|\zeta| > L_0/2$ the amplitude of the vector potential goes to zero with a ramp characterized by a scale length L_r such that $\lambda_0 \ll L_r \ll L_0 \sim k_p^{-1}$. The exact functional form of the ramp is not relevant. The energy of the pulse is $U_c \simeq \pi A_0^2 k_0^2 w_0^2 L_0/4$ and the wakefield behind the pulse is $\phi_c \simeq -(A_0^2/2)\sin(k_pL_0/2)e^{-2\boldsymbol{r}^2/w_0^2}\sin k_p\zeta$. Equating the wakefield amplitude for the pulse train ϕ_{tot} given by Eq. (28) to the one of a single pulse, we obtain that the two are equivalent if

$$a_0 = \sqrt{\frac{8}{3}}A_0. \qquad (29)$$

By substituting the value of a_0 given by Eq. (29) in the expression for U_{tot}, Eq. (26), and comparing U_{tot} with the energy of the single pulse, U_c, we obtain

$$\frac{U_{tot}}{U_c} \simeq 1 + \frac{4\pi^2}{3}\frac{k_p^2}{k_0^2}\frac{N^2}{(k_pL_0)^2} \gtrsim 1. \qquad (30)$$

We notice that, even though the wakefield generated by the stack of pulses is equivalent to the one generated by a single coherent pulse, the total energy of the combination of pulses is more than the one of the coherent pulse. The loss in the efficiency of the combination is related to finite pulse length effects, and is sensitive to the details of the longitudinal pulse envelope. However, for physically relevant parameters, the quantity $\eta = (4\pi^2/3)(k_p/k_0)^2[N^2/(k_pL_0)^2]$ is small. In fact, for a resonant flattop pulse $k_pL_0 = \pi$, and the condition $\ell_0 \gtrsim 2\lambda_0$ limits the maximum number of pulses to $N \lesssim (k_0/k_p)/4$, and so $\eta \lesssim 0.08$. In a 10 GeV LPA stage ($k_0/k_p \sim 100$) the maximum number of pulses in the train would be $N \lesssim 25$, with an energy per pulse of $\gtrsim 1.3$ J. The overall number of pulses in the train can be doubled (and so the energy of each pulse halved) by using polarization multiplexing.

A numerical example of wakefield generated by the incoherent pulse stacking is presented in Fig. (3). In Fig. (3) (a) we show (black dashed line) the normalized laser field envelope for a single (coherent) flat-top laser pulse with $A_0 = 1.5, k_0/k_p = 150, k_pL_0 = \pi$. The red plot is the laser field generated by stacking longitudinally 37 pulses with $a_0 = \sqrt{8/3}A_0 \simeq 2.45, \ell_0 = 2\lambda_0$. The laser phases for the 37 pulses are random. In Fig. (3)
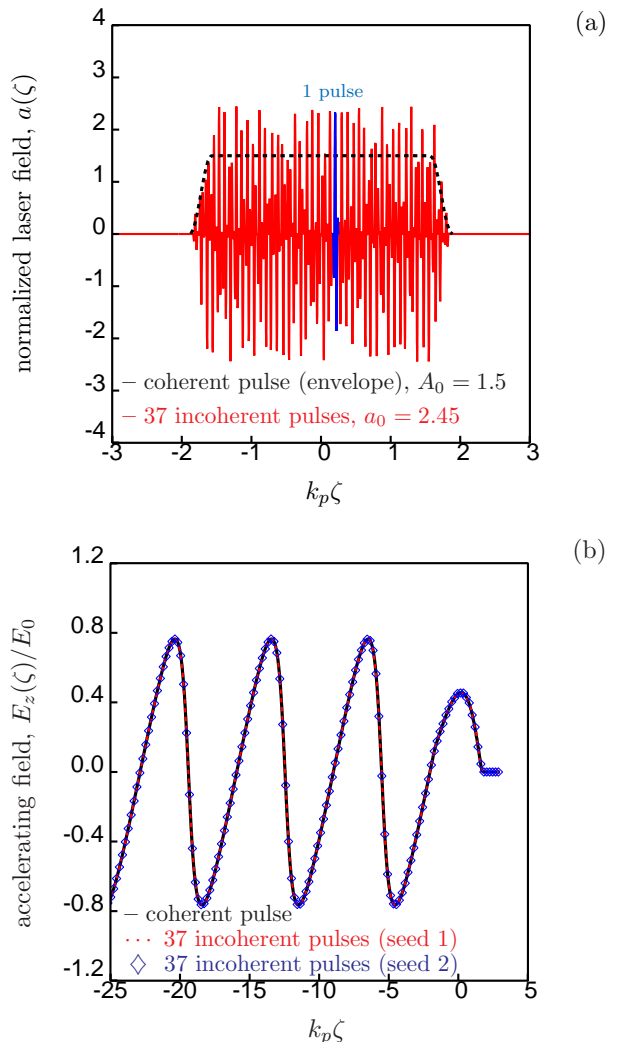
FIG. 3. (a) Normalized laser field envelope for a single (coherent) flat-top laser pulse with $A_0 = 1.5, k_0/k_p = 150, k_pL_0 = \pi$ (black dashed line). The red plot is the laser field generated by stacking longitudinally 37 pulses with $a_0 = \sqrt{8/3}A_0 \simeq 2.45, \ell_0 = 2\lambda_0$. The laser phases for the 37 pulses are random. (b) Lineout of the longitudinal accelerating field generated by the coherent pulse (black line) and by the incoherent stacking of laser pulses for two different set of values of the laser phases (dotted red line and blue diamonds).

(b) we show the lineout of the longitudinal accelerating field, $E_z(\zeta)/E_0$, generated by the coherent pulse (black line) and by the incoherent stacking of laser pulses for two different set of values of the laser phases (dotted red line and blue diamonds). As expected, we have that the wakefield from incoherent combination equals the one from the single coherent pulse. The energy of the incoherent combination exceeds the energy of the coherent pulse by $\sim 8\%$ in agreement with Eq. (30).

IV.   MOSAIC OF INCOHERENT LASER BEAMLETS

As a third example of driving a wakefield with incoherently combined laser pulses, we consider a collection of short and narrow laser beamlets placed side-by-side, both longitudinally and transversally, tiling a prescribed volume. Each pulse has high (relativistic) peak intensity but low energy owing to the limited spatial extent of the beamlets. The domain to be tiled (cylinder in 3D or square in 2D) is given by $|\zeta| < L_0$, and $r = \sqrt{x^2 + y^2} < W_0$, in 3D, or $|x| < W_0$, in 2D Cartesian geometry. This scheme can be seen as the generalization to the transverse dimensions of the one presented in the previous section. For simplicity, we will restrict our analysis to the 2D Cartesian geometry. The generalization to 3D is straightforward. In this scheme the pulses are initially organized into a 2D grid of $N_z \times N_x$ points, then, at each location, two laser beamlets with orthogonal polarization can be accommodate (polarization multiplexing). The total number of beamlets is then $N = N_z \times N_x \times 2$. All the laser beamlets have the same amplitude of the normalized vector potential, a_0, wavelength, $\lambda_0 = 2\pi/k_0$, pulse length, ℓ_0, spot diameter, d_0. The longitudinal and transverse coordinates of the centroid of the beamlets are, $\zeta_{0,i} = -L_0/2 + \ell_0/2 + \ell_0(i-1)$, for $i = 1, \cdots, N_z$, and $x_{0,j}^{(k)} = -W_0 + d_0/2 + d_0(j + k/2 - 1)$ for $j = 1, \cdots, N_x$ and $k = 0, 1$, where k is the polarization index (e.g., $k = 0$ for the in-plane polarization, $k = 1$ for the out-of-plane polarization). The laser field for each beamlet is non-zero only over the domain defined by $|\zeta - \zeta_{0,i}| < \ell_0/2$ and $|x - x_{0,j}^{(k)}| < d_0/2$, and so beamlets with the same polarization do not overlap. The form of the laser vector potential for the pulses at $s = 0$ is,

$$a_{\perp,ij}^{(k)}(\zeta, x) = a_0 \, f_\perp\left(\frac{x - x_{0,j}^{(k)}}{d_0}\right) f_\parallel\left(\frac{\zeta - \zeta_{0,i}}{\ell_0}\right)$$
$$\times \cos[k_0(\zeta - \zeta_{0,i}) + \varphi_{i,j,k}], \qquad (31)$$

where $\varphi_{i,j,k}$ is the laser phase (different for each laser), and $f_\perp(y)$, $f_\parallel(y)$ are compact support functions that vanishes for $|x| > 1/2$. In the following we will assume $f_\perp = f_\parallel = f$, where f is the one defined in Eq. (24).

The guiding of this incoherent combination of laser pulses over distances much longer compared to the Rayleigh length of the single beamlets, namely $Z_R \sim \pi d_0^2/\lambda_0$, can be achieved by a plasma channel with a constant density, $n(x) = n_0$, up to a distance $R \sim W_0$ from the axis, and then, for $|x| > R$, a steep plasma wall, for instance $n(x) = n_0 + \rho(|x| - R)^8$, where ρ is a parameter that sets the steepness of the wall. The optimal value of both R and ρ is chosen via numerical simulations. During propagation the single beamlets diffract but their energy is reflected by the plasma walls. Because of multiple reflections, and interference between fields of different beamlets, we expect the total electromagnetic radiation driving the wake to have a complex pattern. Another consequence of multiple reflections, and of the fact that
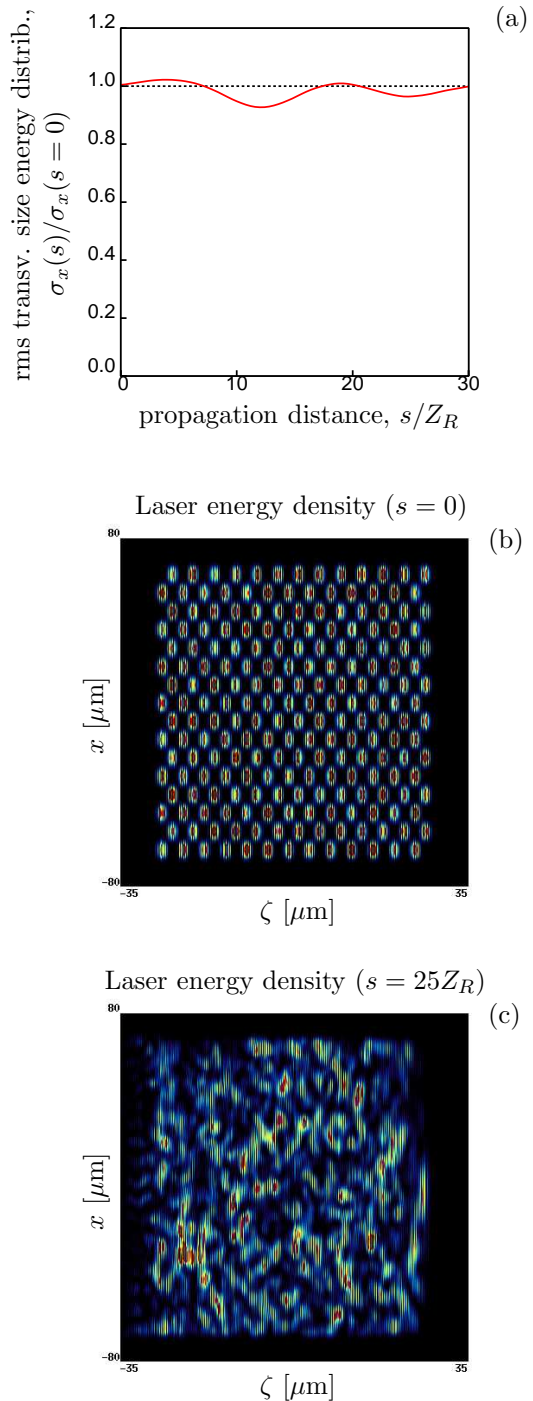
FIG. 4. (a) Evolution of the rms transverse size of the energy distribution, $\sigma_x(s)$, for a combinations of $208 = 13 \times 8 \times 2$ beamlets with $a_0 = 1.5$, $\ell_0 = 4$ μm, $d_0 = 15$ μm, $\lambda_0 = 0.8$ μm. The background plasma density is $n_0 = 0.9 \cdot 10^{17}$ cm^{-3}. The beamlets are tiling a 2D domain with $L_0 = 55$ μm, and $2W_0 = 144$ μm. (b) Snapshot of the laser energy density at the beginning of the simulation, and (c) after some propagation distance in the plasma.

each beamlet is characterized by a typical (finite) diffrac-

tion angle, is the increase of the effective driver length, implying a slow decrease of the accelerating field induced by the loss of resonance of the driver.

In Fig. (4) (a) we show, as an example, the evolution of the rms transverse size of the energy distribution, $\sigma_x(s)$, for a combinations of $208 = 13 \times 8 \times 2$ beamlets with $a_0 = 1.5$, $\ell_0 = 4 \ \mu m$, $d_0 = 15 \ \mu m$, $\lambda_0 = 0.8 \ \mu m$. The background plasma density is $n_0 = 0.9 \cdot 10^{17} \ cm^{-3}$. The beamlets are tiling a 2D domain with $L_0 = 55 \ \mu m$, and $2W_0 = 144 \ \mu m$. We see that the laser energy from the combination is well guided over distances significantly longer than the Rayleigh length of the beamlets. Fig. (4) (b,c) show snapshots of the laser energy density at the beginning of the simulation (b), and after some propagation distance in the plasma (c), where the laser field exhibits a clear incoherent pattern.

To simplify the analytical description of the system, we will assume $k_p\ell_0 \ll 1$ (short pulse compared to the plasma wavelength), $\ell_0 \gtrsim 2\lambda_0$, and $w_0/\ell_0 \gg 1$. An esti-

mate of the single pulse energy is give by

$$U_{ij}^{(k)} \simeq \int d\zeta \int dx \left(\frac{\partial a_{\perp,ij}^{(k)}}{\partial \zeta} \right)^2$$
$$\simeq \frac{9}{128} a_0^2 k_0^2 d_0 \ell_0 \left[1 + \frac{4\pi^2}{3} \frac{1}{(k_0\ell_0)^2} \right]. \quad (32)$$

Since the beamlets are (initially) non-overlapping, the total energy of the combination is

$$U_{tot} = \sum_{j=1}^{N} U_j$$
$$\simeq \frac{9}{128} N a_0^2 k_0^2 d_0 \ell_0 \left[1 + \frac{4\pi^2}{3} \frac{1}{(k_0\ell_0)^2} \right]$$
$$\simeq \frac{9}{32} a_0^2 k_0^2 W_0 L_0 \left[1 + \frac{4\pi^2}{3} \frac{k_p^2}{k_0^2} \frac{N_z^2}{(k_pL_0)^2} \right]. \quad (33)$$

As shown in the previous sections, in the limit $a_0 \lesssim 1$ (linear wakefield), and by using the quasi-static approximation, we can obtain an estimate of the wakefield amplitude at early times during propagation, when the structure of the total electromagnetic fields of the beamlets is still reasonably simple. In particular, behind the region occupied by the drive lasers, the longitudinal accelerating fields reads

$$E_{z,tot}(\zeta, x)/E_0 \simeq \frac{3}{32} a_0^2 (k_p\ell_0) \sum_{i=1}^{N_z} \sum_{j=1}^{N_x} \sum_{k=0}^{1} f^2 \left(\frac{x - x_{0,j}^{(k)}}{d_0} \right) \left[\cos(k_p\zeta)\cos(k_p\zeta_{0,i}) + \sin(k_p\zeta)\sin(k_p\zeta_{0,i}) \right]. \quad (34)$$

In this calculation we neglected the terms of the wakefield depending on the laser phases $\varphi_{i,j,k}$ since, as shown in the previous section, already for very short pulses, namely $\ell_0/\lambda_0 \gtrsim 3$, their contribution is negligible. We notice that, in Eq. (34), $\sum_{i=0}^{N_z} \cos k_p\zeta_{0,i} \simeq (2/k_p\ell_0)\sin(k_pL_0/2)$, and that $\sum_{i=0}^{N_z} \sin k_p\zeta_{0,i} \simeq 0$. We also notice that the dependence of E_z on x is modulated by the function $g(x) \equiv \sum_{j=1}^{N_x} \sum_{k=0}^{1} f^2[(x - x_{0,j}^{(k)})/d_0]$, whose average value, which depends on the particular disposition of the beamlets, the dimensionality (2D Cartesian), and the particular choice of the transverse envelope shape for the beamlets. For Eq. (24), the average of $g(x)$ is $3/4$. As a consequence, the mean amplitude of E_z far from the plasma walls is

$$E_{z,tot}(\zeta, |x| \ll R)/E_0 \simeq \frac{9}{64} a_0^2 \sin\left(\frac{k_pL_0}{2} \right) \cos k_p\zeta. \quad (35)$$

We compare the wakefield generated by the combination of beamlets with the one generated by a single (coherent) laser pulse with amplitude A_0, wavenumber k_0. The pulse has a longitudinal flattop intensity profile of length L_0, and a super-Gaussian transverse intensity pro-

file, namely $a_c(\zeta, x) = A_0 \exp[-(x/W_0)^{14}]\cos(k_0\zeta)$ for $|\zeta| < L_0/2$. For $|\zeta| > L_0/2$ the amplitude of the vector potential goes to zero with a ramp characterized by a scale length L_r such that $\lambda_0 \ll L_r \ll L_0 \sim k_p^{-1}$. We notice that the intensity profile is transversally constant for $|x| \lesssim W_0$, as is the transverse profile for the incoherent combination case. The energy of the coherent pulse is $U_c \simeq A_0^2 k_0^2 W_0 L_0$, and the on-axis accelerating field behind the pulse is $E_{z,c}(\zeta, x = 0)/E_0 \simeq \frac{A_0^2}{2} \sin\left(\frac{k_pL_0}{2} \right) \cos k_p\zeta$. Equating the field amplitude for the beamlets, $E_{z,tot}$, given by Eq. (35) to the one of a single pulse, we obtain that the two are equivalent if

$$a_0 = \frac{4\sqrt{2}}{3} A_0. \quad (36)$$

By substituting the value of a_0 given by Eq. (36) into the expression for U_{tot}, Eq. (33), and comparing U_{tot} with the energy of the single pulse, U_c, we obtain

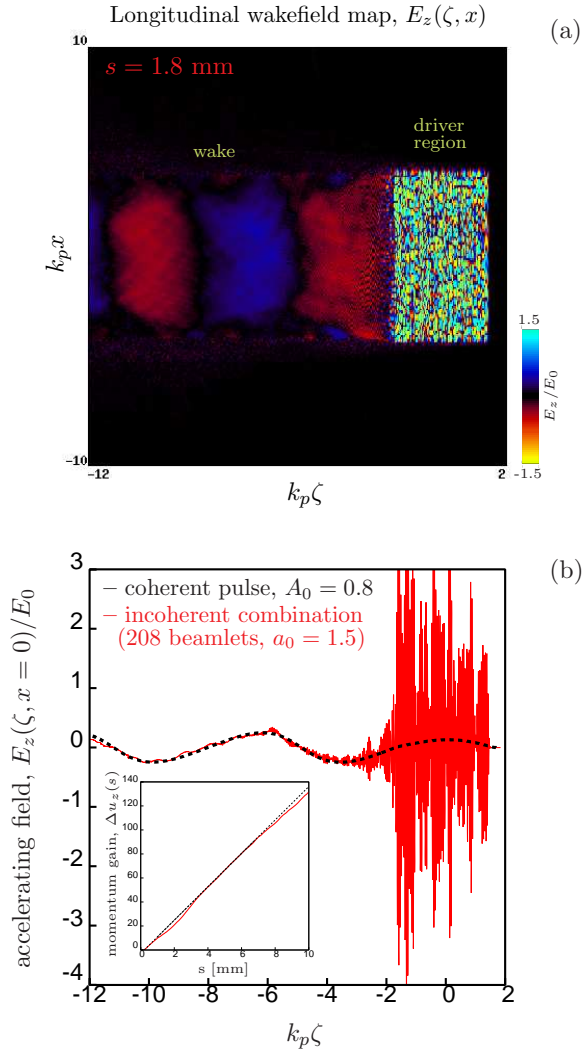$$\frac{U_{tot}}{U_c} \simeq 1 + \frac{4\pi^2}{3} \frac{k_p^2}{k_0^2} \frac{N_z^2}{(k_pL_0)^2} \gtrsim 1. \quad (37)$$

structure that is localized in space and time to a volume $\sim \lambda_p^3$).

To illustrate the physics, we considered three different combination schemes, namely, spectral combining, pulses stacking, and a mosaic of beamlets. The aim of these schemes is to deliver in a suitable spatial volume a certain amount of electromagnetic energy obtained from multiple, low-energy laser beams. For each incoherent combination scheme examined, we characterized the wakefield amplitude and compared it to that generated by a single (coherent) laser pulse with the same rms length and width. In particular, we determined under which conditions the wakefield generated by the incoherent combination is equivalent to that generated by the single coherent pulse and we compared the total energy for each case. More specifically, we find that, for the wavelength combination scheme, the wakefield amplitude excited by the combination can be equal to that generated by a single (coherent) pulse, and the energy of the combination equals the energy of the single pulse, i.e., the incoherent combination scheme is as efficient as the coherent one in generating the wakefield. For the cases of the pulse stack and the mosaic of beamlets, we find that, even though the wakefield amplitude of the combination equals the one of a single pulse, the total energy of the combination exceeds the one of a single pulse. However, the loss in the efficiency is generally limited to a few percent.

For each combination scheme we discussed the main limitations. These limitations include dispersive lengthening of the collection of pulses, limitations imposed by geometry, and limitations due to laser technology. For example, the maximum number of pulses that can be accommodated in the spectral combining scheme depends on the maximum bandwidth, the available frequencies, and the plasma wavelength for a given density. The three combination schemes discussed in this paper serve as illustrative examples and should not be considered as an optimized configuration. One can readily envision other possible schemes for the incoherent combination of laser pulses. For instance, some features of the approaches discussed in this paper can be used in conjunction, e.g., the wavelength combination approach can be used together with the pulse train scheme or with the mosaic of beamlets. This would allow increasing the overall number of beams to use in the combination and so further reduce the energy of each pulse.

Virtually all applications of LPAs would benefit greatly from an increase in laser repetition rate and average power. These applications range from drivers for advanced light sources (e.g., short-wavelength free-electron lasers) to large-scale colliders for high-energy physics. As an example, the laser requirements for a LPA-based collider are extremely challenging, requiring high efficiency lasers with repetition rates on the order of ten kHz, and average powers on the order of hundreds of kW. Present high power, short pulse laser systems based on Ti-sapphire are limited to an average power on the order of hundreds of W. One approach to the next generation of laser drivers for LPAs that is widely being researched is the coherent combination of a large number of fiber lasers. Coherent combination of lasers entails several technical challenges including control of the laser phase, spatial combination, and precise pulse timing and synchronization (to within a fraction of a laser wavelength). Our study, however, has shown that coherent combination is not required for an LPA. Since no control over the relative laser phases is imposed, we expect that fundamental requirements to achieve incoherent combination are more relaxed compared to coherent combination, thereby enabling a technologically simpler path for design of high-peak power, high-average power, high-repetition rate LPAs and associated applications.

[1] E. Esarey, C. B. Schroeder, and W. P. Leemans, Rev. Mod. Phys. **81**, 1229 (2009).

[2] S. M. Hooker, Nature Photon. **7,** 775 (2013).

[3] W. P. Leemans, B. Nagler, A. J. Gonsalves, C. Tóth, K. Nakamura, C. G. R. Geddes, E. Esarey, C. B. Schroeder, and S. M. Hooker, Nature Phys. **2**, 696 (2006).

[4] X. Wang, R. Zgadzaj, N. Fazel, Z. Li, S. A. Yi, X. Zhang, W. Henderson, Y.-Y. Chang, R. Korzekwa, H.-E. Tsai, C.-H. Pai, H. Quevedo, G. Dyer, E. Gaul, M. Martinez, A. C. Bernstein, T. Borger, M. Spinks, M. Donovan, V. Khudik, G. Shvets, T. Ditmire, and M. C. Downer, Nat. Commun. **4,** 1988 (2013).

[5] E. Esarey, R. F. Hubbard, W. P. Leemans, A. Ting, and P. Sprangle, Phys. Rev. Lett. **79**, 2682 (1997).

[6] J. Faure, C. Rechatin, A. Norlin, A. Lifschitz, Y. Glinec, and V. Malka, Nature **444**, 737 (2006).

[7] S. Bulanov, N. Naumova, F. Pegoraro, and J. Sakai, Phys. Rev. E **58**, R5257 (1998).

[8] C. G. R. Geddes, K. Nakamura, G. R. Plateau, Cs. Tóth, E. Cormier-Michel, E. Esarey, C. B. Schroeder, J. R. Cary, and W. P. Leemans, Phys. Rev. Lett. **100**, 215004 (2008).

[9] A. J. Gonsalves, K. Nakamura, C. Lin, D. Panasenko, S. Shiraishi, T. Sokollik, C. Benedetti, C. B. Schroeder, C. G. R. Geddes, J. van Tilborg, J. Osterhoff, E. Esarey, Cs. Tóth, and W. P. Leemans, Nature Phys. **7**, 862 (2011).

[10] O. Lundh, J. Lim, C. Rechatin, L. Ammoura, A. Ben-Ismaïl, X. Davoine, G. Gallot, J-P. Goddet, E. Lefebvre, V. Malka, and J. Faure, Nature Phys. **7**, 219-222 (2011).

[11] G. R. Plateau, C. G. R. Geddes, D. B. Thorn, M. Chen, C. Benedetti, E. Esarey, A. J. Gonsalves, N. H. Matlis, K. Nakamura, C. B. Schroeder, S. Shiraishi, T. Sokollik, J. van Tilborg, Cs. Tóth, S. Trotsenko, T. S. Kim, M. Battaglia, Th. Stöhlker, and W.P. Leemans, Phys. Rev. Lett. **109**, 064802 (2012).

[12] C. Lin, J. van Tilborg, K. Nakamura, A. J. Gonsalves, N. H. Matlis, T. Sokollik, S. Shiraishi, J. Osterhoff, C. Benedetti, C. B. Schroeder, Cs. Tóth, E. Esarey, and W.P. Leemans, Phys. Rev. Lett. **108,** 094801 (2012).

[13] A. Buck, M. Nicolai, K. Schmid, C. M. S. Sears, A. Sävert, J. M. Mikhailova, F. Krausz, M. C. Kaluza, and L. Veisz, Nature Phys. **7**, 543 (2011).

[14] W. P. Leemans, C. G. R. Geddes, J. Faure, Cs. Tóth, J. van Tilborg, C. B. Schroeder, E. Esarey, G. Fubiani, D. Auerbach, B. Marcelis, M. A. Carnahan, R. A. Kaindl, J. Byrd, and M. C. Martin , Phys. Rev. Lett. **91**, 074802 (2003).

[15] A. Rousse, K. T. Phuoc, R. Shah, A. Pukhov, E. Lefebvre, V. Malka, S. Kiselev, F. Burgy, J.-P. Rousseau, D. Umstadter, and D. Hulin, Phys. Rev. Lett. **93**, 135005 (2004).

[16] M. Fuchs, R. Weingartner, A. Popp, Z. Major, S. Becker, J. Osterhoff, I. Cortrie, B. Zeitler, R. Hörlei, G. D. Tsakiris, U. Schramm, T. P. Rowlands-Rees, S. M. Hooker, D. Habs, F. Krausz, S. Karsch, and F. Grüner, Nature Phys. **5**, 826 (2009).

[17] A. R. Maier, A. Meseck, S. Reiche, C. B. Schroeder, T. Seggebrock, and F. Grüner, Phys. Rev. X **2** 031019 (2012).

[18] Z. Huang, Y. Ding, and C. B. Schroeder, Phys. Rev. Lett. **109**, 204801 (2012).

[19] W. P. Leemans and E. Esarey, Phys. Today **62**, 44 (2009).

[20] C. B. Schroeder, E. Esarey, C. G. R. Geddes, C. Benedetti, and W. P. Leemans, Phys. Rev. ST Accel. Beams **13**, 101301 (2010).

[21] K. Nakajima, A. Deng, X. Zhang, B. Shen, J. Liu, R. Li, Z. Xu, T. Ostermayr, S. Petrovics, C. Klier, K. Iqbal, H. Ruhl, and T. Tajima, Phys. Rev. ST Accel. Beams **14**, 091301 (2011).

[22] C. B. Schroeder, E. Esarey, and W. P. Leemans, Phys. Rev. ST Accel. Beams **15**, 051301 (2012).

[23] W. P. Leemans, J. Daniels, A. Deshmukh, A. J. Gonsalves, A. Magana, H. S. Mao, D. E. Mittelberger, K. Nakamura, J. R. Riley, D. Syversrud, C. Toth, N. Ybarrolaza, in Proceedings of PAC2013 (JaCoW, 2013), p. THYAA1.

[24] http://www.acceleratorsamerica.org/report/

[25] J. W. Dawson, J. K. Crane, M. J. Messerly, M. A. Prantil, P. H. Pax, A. K. Sridharan, G. S. Allen, D. R. Drachenberg, H. H. Phan, J. E. Heebner, C. A. Ebbers, R. J. Beach, E. P. Hartouni, C. W. Siders, T. M. Spinka, C. P. J. Barty, A. J. Bayramian, L. C. Haefner, F. Albert, W. H. Lowdermilk, A. M. Rubenchik, and R. E. Bonanno, AIP Conf. Proc. **1507**, 147 (2012).

[26] G. Mourou, B. Brocklesby, T. Tajima, and J. Limpert, Nature Photon. **7**, 258 (2013).

[27] G. A. Mourou, D. Hulin,and A. Galvanauskas, AIP Conf. Proc. **827**, 152 (2006).

[28] J. Bourderionnet, C. Bellanger, J. Primot, and A. Brignon, Opt. Express **19**, 17053 (2011).

[29] L. Daniault, M. Hanna, D. N. Papadopoulos, Y. Zaouter, E. Mottay, F. Druon, and P. Georges, Opt. Lett. **36**, 4023 (2011).

[30] A. Klenke, E. Seise, S. Demmler, J. Rothhardt, S. Breitkopf, J. Limpert, and A. Tünnermann, Opt. Express **19**, 24280 (2011).

[31] T.Y. Fan, IEEE Journal of Selected topics in quantum electronics **11**, 567 (2005).

[32] C. B. Schroeder, C. Benedetti, E. Esarey, and W. P. Leemans, Phys. Rev. Lett. **106**, 135002 (2011).

[33] C. B. Schroeder, C. Benedetti, E. Esarey, J. van Tilborg, and W.P. Leemans, Phys. Plasmas **18**, 083103 (2011).

[34] C. Benedetti, A. Sgattoni, G. Turchetti, and P. Londrillo, IEEE Transactions on plasma science **36**, 1790 (2008).

[35] C. Benedetti, P. Londrillo, V. Petrillo, L. Serafini, A. Sgattoni, P. Tomassini, G. Turchetti, Nucl. Instr. and Meth. A **608**, 94 (2009).